J Appl Biomed
DOI: 10.32725/jab.2023.009
journal homepage: http://jab.zsf.jcu.cz

Journal of Applied Biomedicine

Original research article

Antioxidant action of xanthine oxidase inhibitor febuxostat protects the liver and blood vasculature in SHRSP5/Dmcr rats

Mai Kakimoto [1], Moe Fujii [1], Ikumi Sato [1], Koki Honma [1], Hinako Nakayama [1], Sora Kirihara [1], Taketo Fukuoka [2], Shang Ran [1], Satoshi Hirohata [3], Kazuya Kitamori [4], Shusei Yamamoto [1, 3], Shogo Watanabe [3] *

[1] *Okayama University, Graduate School of Health Sciences, Department of Medical Technology, 2-5-1, Shikata-cho, Kita-ku, Okayama-shi, Okayama 700-8558, Japan*
[2] *Okayama University, Faculty of Health Sciences, Department of Medical Technology, 2-5-1, Shikata-cho, Kita-ku, Okayama-shi, Okayama, 700-8558, Japan*
[3] *Okayama University, Academic Field of Health Science, 2-5-1, Shikata-cho, Kita-ku, Okayama-shi, Okayama, 700-8558, Japan*
[4] *Kinjo Gakuin University, College of Human Life and Environment, 2-1723, Omori, Moriyama-ku, Nagoya-shi, Aichi, 463-8521, Japan*

Abstract
Background: Xanthine oxidase (XO) generates reactive oxygen species during uric acid production. Therefore, XO inhibitors, which suppress oxidative stress, may effectively treat non-alcoholic steatohepatitis (NASH) and atherosclerosis via uric acid reduction. In this study, we examined the antioxidant effect of the XO inhibitor febuxostat on NASH and atherosclerosis in stroke-prone spontaneously hypertensive 5 (SHRSP5/Dmcr) rats.
Methods: SHRSP5/Dmcr rats were divided into three groups: SHRSP5/Dmcr + high-fat and high-cholesterol (HFC) diet [control group, n = 5], SHRSP5/Dmcr + HFC diet + 10% fructose (40 ml/day) [fructose group, n = 5], and SHRSP5/Dmcr + HFC diet + 10% fructose (40 ml/day) + febuxostat (1.0 mg/kg/day) [febuxostat group, n = 5]. Glucose and insulin resistance, blood biochemistry, histopathological staining, endothelial function, and oxidative stress markers were evaluated.
Results: Febuxostat reduced the plasma uric acid levels. Oxidative stress-related genes were downregulated, whereas antioxidant factor-related genes were upregulated in the febuxostat group compared with those in the fructose group. Febuxostat also ameliorated inflammation, fibrosis, and lipid accumulation in the liver. Mesenteric lipid deposition decreased in the arteries, and aortic endothelial function improved in the febuxostat group.
Conclusions: Overall, the XO inhibitor febuxostat exerted protective effects against NASH and atherosclerosis in SHRSP5/Dmcr rats.

Keywords: Anti-inflammatory; Atherosclerosis; Febuxostat; Non-alcoholic steatohepatitis (NASH); Oxidative stress; Uric acid

Highlights:
- Oxidative stress aggravates non-alcoholic steatohepatitis and atherosclerosis.
- The XO inhibitor febuxostat improves insulin resistance and inflammation.
- Febuxostat protects against non-alcoholic steatohepatitis and atherosclerosis.

Abbreviations:
ACh: Acetylcholine; ALT: Alanine aminotransferase; AST: Aspartate; aminotransferase; AUC: Area under the curve; CAT: Catalase; CYP2E1: Cytochrome P450 2E1; DMSO: Dimethyl sulfoxide; DW: Distilled water; GPx-1: Glutathione peroxidase 1; HDL: High-density lipoprotein; HFC: High-fat and high-cholesterol; HOMA-IR: Homeostasis model assessment of insulin resistance; IRS-1: Insulin receptor substrate-1; ITT: Insulin tolerance test; LDL: Low-density lipoprotein; MCP-1: Monocyte chemoattractant protein-1; MDA: Malondialdehyde; NAFLD: Non-alcoholic fatty liver disease; NAS: Non-alcoholic fatty liver disease activity scores; NASH: Non-alcoholic steatohepatitis; NFκB: Nuclear factor-kappa B; NO: Nitric oxide; NOX2: Nicotinamide adenine dinucleotide phosphate oxidase 2; OGTT: Oral glucose tolerance test; PBS: Phosphate-buffered saline; P-C: Portal to central; PGF2α: Prostaglandin F2 alpha; P-P: Portal to portal; ROS: Reactive oxygen species; RT-PCR: Reverse transcription-polymerase chain reaction; SBP: Systolic blood pressure; SHRSP5/Dmcr: Stroke-prone spontaneously hypertensive 5; SP: Stroke-prone; TNF-α: Tumor necrosis factor-α; XO: Xanthine oxidase

* **Corresponding author:** Shogo Watanabe, Okayama University, Academic Field of Health Science, 2-5-1, Shikata-cho, Kita-ku, Okayama-shi, Okayama, 700-8558, Japan; e-mail: watanabe1224@okayama-u.ac.jp
http://doi.org/10.32725/jab.2023.009

Submitted: 2022-12-15 • Accepted: 2023-04-25 • Prepublished online: 2023-05-22
J Appl Biomed 21/2: 80–90 • EISSN 1214-0287 • ISSN 1214-021X

Introduction

Non-alcoholic fatty liver disease (NAFLD) can progress to non-alcoholic steatohepatitis (NASH), which in turn leads to cirrhosis and liver cancer; therefore, early treatment is required (Argo and Caldwell, 2009; Cohen et al., 2011). The prevalence of NASH increases in association with lifestyle-related diseases, such as diabetes, obesity, and metabolic syndrome, underscoring the urgent need for effective treatment options (Wei et al., 2015). However, the pathogenesis of NASH remains poorly understood, although several factors may contribute to its development. Fructose increases the risk of NASH by inducing insulin resistance and promoting hepatic lipid accumulation (Jegatheesan and De Bandt, 2017; Lin et al., 2016; Shuprovych et al., 2011; Softic et al., 2016), suggesting the causal involvement of uric acid (Mosca et al., 2017). In many epidemiological studies, cardiovascular disease has been positively correlated with uric acid levels (Ndrepepa, 2018; Verdecchia et al., 2000; Zhang et al., 2016). In addition, uric acid affects the vascular endothelium and causes atherosclerosis development (Khosla et al., 2005; Mishima et al., 2016). However, whether uric acid levels are a direct risk factor for atherosclerosis remains elusive because these levels are affected by various factors associated with the development of atherosclerosis, such as diabetes, obesity, and hypertension (Feig et al., 2008). In this context, xanthine oxidase (XO) inhibitors may exert protective effects against NASH and atherosclerosis via uric acid reduction (Nakatsu et al., 2015). XO functions in various organs, such as the liver, kidney, and vascular tissue, and produces reactive oxygen species (ROS) during uric acid production. Therefore, XO inhibitors that suppress oxidative stress may effectively protect against NASH and atherosclerosis (Khosla et al., 2005; Nakatsu et al., 2015).

In this study, we tested the novel XO inhibitor, febuxostat, which is more selective and potent than other XO inhibitors (Xu et al., 2021). The effectiveness of febuxostat in treating NASH and atherosclerosis may improve the prognosis of NASH, as there is currently no effective treatment in clinical practice. Therefore, we examined the antioxidant effects of febuxostat against NASH and atherosclerosis in stroke-prone spontaneously hypertensive 5 rats (SHRSP5/Dmcr), which have a pathology similar to that of human NASH, with high fructose-induced elevated uric acid and oxidative stress.

Materials and methods

Animals and diets

We used male SHRSP5/Dmcr rats, a newly established stroke-prone spontaneously hypertensive rat model, for the experiments. SHRSP5/Dmcr rats fed a high-fat and high-cholesterol (HFC) diet have traits similar to those of human patients with NASH (Kitamori et al., 2012). The 13-week-old male SHRSP5/Dmcr rats ($n = 15$) were obtained from the Disease Model Cooperative Research Association (Kyoto, Japan). At 14–26 weeks of age, the rats were divided into three groups: SHRSP5/Dmcr rats + HFC diet (control group, $n = 5$), SHRSP5/Dmcr rats + HFC diet + 10% fructose (fructose group, $n = 5$), and SHRSP5/Dmcr rats + HFC diet + 10% fructose + febuxostat (febuxostat group, $n = 5$). During the first week, the rats consumed water and a stroke-prone (SP) diet *ad libitum* to acclimatize to the experiment. At 14 weeks of age, the SP diet (protein 20.8%, fat 4.8%, fiber 3.2%, ash 5.0%, moisture 8.0%, and carbohydrate 58.2%) was changed to an HFC diet (SP diet 68%, palm oil 25%, cholesterol 5%, and cholic acid 2%). The HFC diet was obtained from the Funabashi Farm (Funabashi, Japan) (Kitamori et al., 2012). From 14 weeks of age, the control group was provided water *ad libitum*, and the fructose and febuxostat groups were loaded with 100 g/l (10%) fructose at 40 ml/day. Febuxostat was dissolved in phosphate-buffered saline (PBS; 10 mM, pH 7.4) and 6% dimethyl sulfoxide (DMSO) and administered intraperitoneally. The dosage of febuxostat was fixed at 1 mg/kg/day. A food intake of 900–1000 g was provided from 14 to 24 weeks of age to avoid any significant differences among the three groups. Body weights were measured at 14 and 24 weeks of age. Systolic blood pressure (SBP) was measured biweekly in conscious rats using tail-cuff plethysmography (BP-98A; Softron, Tokyo, Japan).

All rats were starved overnight at 25 weeks of age, and the oral glucose tolerance test (OGTT) and insulin tolerance test (ITT) were performed. At 26 weeks, all rats were starved overnight, and endothelial function test, blood sampling, and dissection were performed. Quantitative reverse transcription-polymerase chain reaction (RT-PCR) analysis of the liver and pathological staining of the liver and mesenteric arteries were performed.

Chemical reagents

Pentobarbital sodium (Nacalai Tesque, Inc., Kyoto, Japan) and isoflurane (Mylan, Tokyo, Japan) were used for anesthesia. Oil Red O (O0625, Sigma-Aldrich, Tokyo, Japan) was used as the staining solution. Prostaglandin F2 alpha (PGF2α), acetylcholine (ACh), and papaverine were purchased from Maruishi Pharmaceutical Co., Ltd. (Osaka, Japan), Daiichi Sankyo Co., Ltd. (Tokyo, Japan), and Nichi-Iko Pharmaceutical Co., Ltd. (Toyama, Japan), respectively. D-Fructose and formalin were purchased from FUJIFILM Wako Pure Chemical Corporation (Osaka, Japan). PBS (pH 7.4), DMSO, and D-glucose were purchased from Kanto Chemical Co., Inc. (Tokyo, Japan). Febuxostat ($C_{16}H_{16}N_2O_3S$) was purchased from Tokyo Chemical Industry Co. Ltd. (Tokyo, Japan). Insulin was purchased from Eli Lilly Japan, K.K. (Hyogo, Japan).

Blood and organ analysis

At 26 weeks of age, blood was collected from the right carotid artery of all rats that had been deprived of food and had consumed water *ad libitum* overnight. All rats were anesthetized with an intraperitoneal injection of pentobarbital sodium (46.8 mg/kg). The collected blood was centrifuged at 3000 rpm for 15 min, and the resultant plasma supernatants were maintained at –80 °C until analysis. The levels of aspartate aminotransferase (AST), alanine aminotransferase (ALT), triglycerides, total cholesterol, high-density lipoprotein (HDL) cholesterol, low-density lipoprotein (LDL) cholesterol, uric acid, fasting glucose, and insulin were measured using routine laboratory methods (SRL Inc., Tokyo, Japan). The homeostasis model assessment of insulin resistance (HOMA-IR) was calculated using the following equation (Nosrati et al., 2010): HOMA-IR = [fasting glucose (mg/dl) × fasting insulin (ng/ml)]/22.5.

All rats were euthanized, and the liver and aorta were dissected and weighed. The liver was sectioned for histopathological staining, and the remaining sections were frozen for gene analysis. Hepatic lipid droplets were measured as triglycerides at an outsourced facility (Immuno-Biological Laboratories Co., Ltd., Gunma, Japan). Malondialdehyde (MDA), an oxidative stress marker in the liver, was measured by outsourcing to the Japan Institute for the Control of Aging (Nikken SEIL Co., Ltd., Shizuoka, Japan). The aorta was cut into 2 mm rings to

evaluate the endothelial function, and the mesenteric artery was separated from the mesenteric adipose tissue for Oil Red O staining (Kumazaki et al., 2019; Watanabe et al., 2018).

Glucose and insulin resistance

At 25 weeks of age, OGTT was conducted following an overnight fast, with *ad libitum* access to water. All rats were orally administered glucose (2 g/kg) after anesthetization by isoflurane inhalation using inhalation anesthesia equipment for small animal experiments (NARCOBIT-E: II; Natsume Seisakusho Co., Ltd., Tokyo, Japan). Tail blood was sampled before and at 15, 30, 60, and 120 min after glucose administration to measure the blood glucose levels. The ITT was conducted in the same manner as the OGTT. Insulin (1 U/kg) was intraperitoneally injected into rats following a 6 h fast. Blood glucose levels were determined using a glucose analyzer (Glutest Neo Super; Sanwa Kagaku Kenkyusyo, Nagoya, Japan). Blood glucose responses during the OGTT and ITT were estimated from the area under the curve (AUC) using the trapezoidal method (Matsuura et al., 2015; Wei et al., 2011).

Endothelial function

The endothelial function of the aorta of each rat was measured at the end of the experimental period as previously described (Hosoo et al., 2015). Vasorelaxation was expressed as the percentage of relaxation of the PGF2α-induced constriction. After evaluating the endothelial function using Ach, the aortic rings were completely dilated by adding excess vasorelaxant (1.2 mM papaverine) to confirm that the mesothelium functioned properly.

Histopathological analysis

The livers were fixed in 10% formalin for 48 h, embedded in paraffin, and sliced (4 μm) for histological analysis. The livers were stained with Masson's trichrome to evaluate fibrosis and lipid droplets. NAFLD activity scores (NAS) were calculated according to the NASH Clinical Research Network scoring system (Kleiner et al., 2005), which has been applied to rats fed an HFD (Elias et al., 2009; Kitamori et al., 2012). Steatosis, hepatocyte ballooning, lobular inflammation, and fibrosis were rated according to the following classifications (Ishak et al., 1995; Kleiner et al., 2005): A NAS of ≥5 was correlated with a diagnosis of NASH; a NAS of 3–5 indicated borderline NASH; a NAS of <3 indicated no NASH (Kleiner et al., 2005). Fibrosis was quantified on a scale of 0–6 points using the Ishak staging system (Goodman, 2007; Ishak et al., 1995). All the images were obtained using an all-in-one fluorescence microscope (BZ-X700; KEYENCE, Osaka, Japan). Quantitative analysis of the hepatic fibrosis area was performed using BZ-X Analyzer software.

Oil Red O staining of the mesenteric artery was performed as previously described (Kumazaki et al., 2019; Watanabe et al., 2018). The mesenteric artery was carefully isolated from the intestine and fixed in 10% formalin for 10 min. After washing with distilled water, the tissue was immersed in 60% isopropanol for 1 min, followed by immersion in Oil Red O staining solution (O0625, Sigma-Aldrich, Tokyo, Japan) for 30 min (37 °C), 60% isopropanol for 2 min, and distilled water again.

Quantitative RT-PCR analysis

Total RNA was extracted from the liver (30 mg) using an RNeasy Mini Kit (Qiagen, Hilden, Germany) and subjected to reverse transcription (1000 ng) using the PrimeScript™ RT Reagent Kit (Takara, Shiga, Japan). Quantitative PCR analysis was performed using FastStart Essential DNA Green Master (Roche Diagnostics, Mannheim, Germany) and a LightCycler 96 Instrument system (Roche Diagnostics). GAPDH was used as an internal standard. The designed mRNA primers are listed in Table 1.

Table 1. Designed primers

Gene name	Primer sequence	GenBank accession
CAT	F: 5′-ACAGTTCGTGACCCTCGTGG-3′ R: 5′-GGAATCCCTCGGTCGCTGAA-3′	XM_032903812
GPx-1	F: 5′-GCCTAGCAACCCCTAAGGCA-3′ R: 5′-GGCATCGGGAATGGACGAGA-3′	NM_030826
NOX2	F: 5′-TGGTGTGGTTGGGGCTGAAT-3′ R: 5′-GAGCAACACGCACTGGAACC-3′	NM_023965
CYP2E1	F: 5′-CACCCCCTGGATCCAGCTTT-3′ R: 5′-GGCGCAGTTGATGTCCAGTG-3′	NM_031543
MCP-1	F:5′-CAGATCTCTCTTCCTCCACCACTAT-3′ R: 5′-CAGGCAGCAACTGTGAACAAC-3′	NM_031530
TNF-α	F: 5′-AGGCAACACATCTCCCTCCG-3′ R: 5′-CCATCTTTTTGGGGAGCGCC-3′	NM_012675
NFκB	F: 5′-TTCCCTGAAGTGGAGCTAGGA-3′ R: 5′-CATGTCGAGGAAGACACTGGA-3′	NM_199267
GAPDH	F: 5′-TCAAGAAGGTGGTGAAGCAG-3′ R: 5′-AGGTGGAAGAATGGGAGTTG-3′	NM_017008

Note: F, forward; R, reverse; CAT, catalase; GPx-1, glutathione peroxidase 1; NOX2, nicotinamide adenine dinucleotide phosphate oxidase 2; CYP2E1, cytochrome P450 2E1; MCP-1, monocyte chemoattractant; TNF-α, tumor necrosis factor α; NF-κB, nuclear factor kappa B; GAPDH, Glyceraldehyde 3-phosphate dehydrogenase.

XO activity assay

Hepatic XO activity was measured using a xanthine oxidase activity assay kit (Sigma-Aldrich, Burlington, MA, USA). Frozen liver samples (50 mg) were rapidly homogenized in four volumes of xanthine oxidase assay buffer.

XO activity is reported as nmol/min/ml = milliunit/ml. One milliunit (mU) of XO is defined as the amount of enzyme that catalyzes the oxidation of xanthine, yielding 1.0 μmol of uric acid and hydrogen peroxide per minute at 25 °C.

Statistical analysis

The relevant data are expressed as the mean ± standard error. Statistical analysis was performed using the Kruskal–Wallis test. If a significant difference was found, intergroup comparisons were performed using the Student–Newman–Keuls test. A p-value below 0.05 ($p < 0.05$) was considered significant. If no significant difference was found, it was recorded as N.S. * $p < 0.05$, ** $p < 0.01$ relative to control; † $p < 0.05$, †† $p < 0.01$ relative to fructose group.

Results

Physiological data

Significant weight gain was observed in the fructose group compared to that in the control group; however, febuxostat suppressed fructose-induced weight gain (Fig. 1A). There were significant differences in the SBP between the fructose and febuxostat groups at 19–23 weeks of age; however, a constant transition was maintained (Fig. 1B).

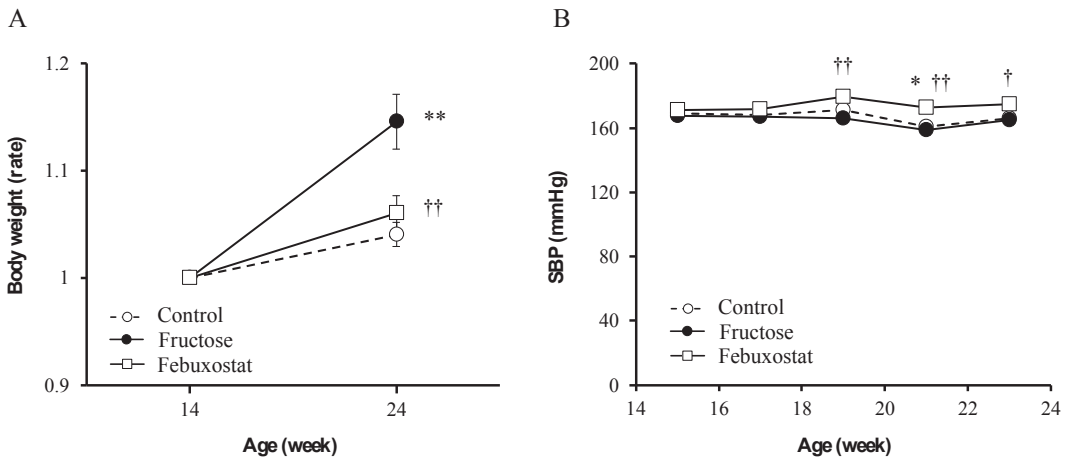

Fig. 1. Physiological data. (**A**) Rate of change in body weight at 14–24 weeks of age. (**B**) Systolic blood pressure (SBP) at 15–23 weeks of age. All data are shown as mean ± standard error (SE); $n = 5$ in each group. * $p < 0.05$, ** $p < 0.01$ vs. control group; † $p < 0.05$, †† $p < 0.01$ vs. fructose group.

Glucose and insulin resistance

Glucose metabolism was evaluated using OGTT, ITT, fasting plasma glucose, fasting plasma insulin, and HOMA-IR. The blood glucose levels determined by the OGTT in the febuxostat group were lower than those in the fructose group at 30, 60, and 120 min (Fig. 2A). The AUC of blood glucose levels determined by OGTT in the febuxostat group was significantly lower than that in the fructose group (Fig. 2B). The ITT did not show significant differences between the two groups; however, the results followed a trend similar to that of the OGTT (Fig. 2C, D). Biochemical analysis revealed that the fasting plasma glucose levels in the febuxostat group were significantly lower than those in the fructose group (Table 2). The fasting plasma insulin level and HOMA-IR, an indicator of insulin resistance, in the febuxostat group were the lowest among the three groups (Table 2).

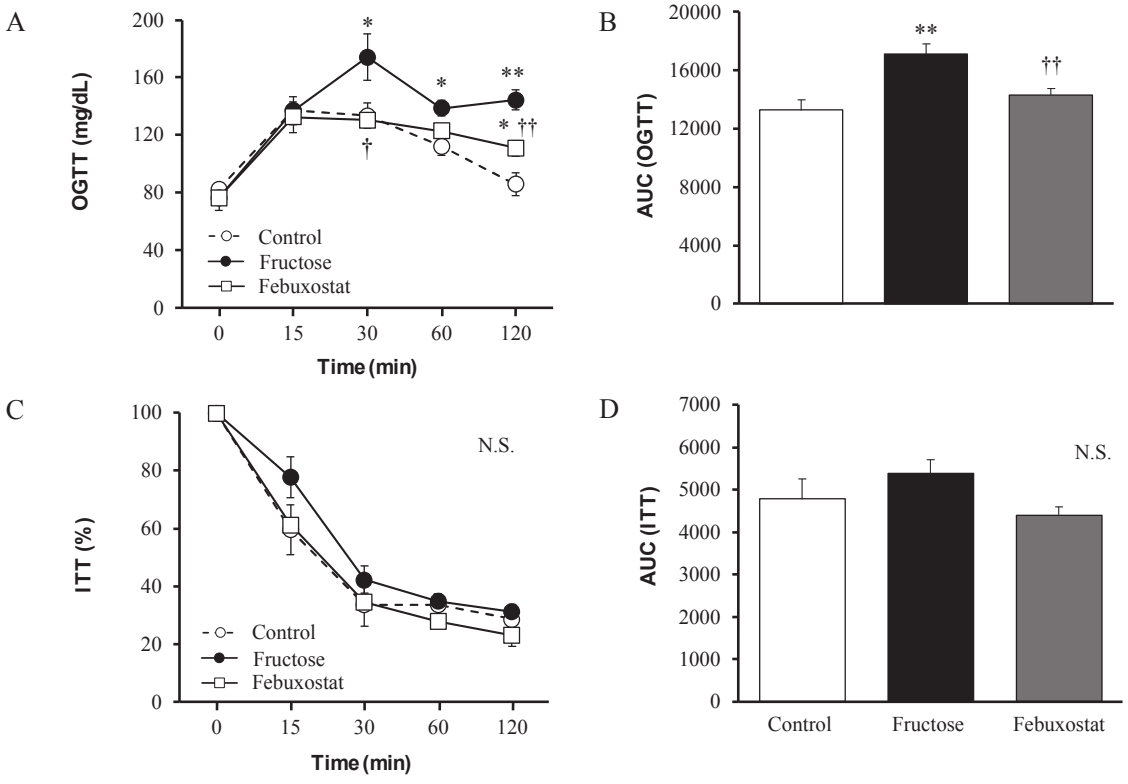

Fig. 2. Glucose and insulin resistance measurement by OGTT and ITT at 25 weeks of age. (**A**) Oral glucose tolerance test (OGTT) blood glucose levels. (**B**) The area under the curve (AUC) in OGTT. (**C**) Blood glucose levels in the insulin tolerance test (ITT). (**D**) AUC in ITT. All data are shown as the mean ± SE; $n = 5$ in each group. * $p < 0.05$, ** $p < 0.01$ vs. control group; † $p < 0.05$, †† $p < 0.01$ vs. fructose group.

Table 2. Results of biochemical analysis of plasma at 26 weeks of age

Parameters	Control	Fructose	Febuxostat
Uric acid (mg/dl)	0.48 ± 0.06	0.98 ± 0.20*	0.54 ± 0.07†
AST (IU/l)	196.8 ± 18.6	255.2 ± 22.1	166.2 ± 12.9††
ALT (IU/l)	91.6 ± 19.6	136.0 ± 14.1	90.4 ± 9.4
Total cholesterol (mg/dl)	126.4 ± 7.5	174.0 ± 3.8**	94.8 ± 7.2**††
HDL-cholesterol (mg/dl)	20.2 ± 0.6	30.8 ± 1.1**	16.0 ± 1.3*††
LDL-cholesterol (mg/dl)	36.2 ± 1.8	40.0 ± 2.3	29.8 ± 2.4††
LDL-/HDL-cholesterol ratio	1.79 ± 0.08	1.30 ± 0.06**	1.87 ± 0.04††
Triglyceride (mg/dl)	18.2 ± 3.6	33.8 ± 8.4	11.2 ± 0.7†
Fasting glucose (mg/dl)	80.2 ± 7.4	205.4 ± 27.3**	73.2 ± 3.1††
Fasting insulin (ng/ml)	1.12 ± 0.10	2.72 ± 1.50	0.44 ± 0.07
HOMA-IR	4.8 ± 1.3	25.9 ± 14.3	2.0 ± 0.6

Note: All data are shown as mean ± standard error (SE); $n = 5$ in each group. * $p < 0.05$, ** $p < 0.01$ vs. Control group, † $p < 0.05$, †† $p < 0.01$ vs. Fructose group; N.S: not significant; AST, aspartate aminotransferase; ALT, alanine aminotransferase; HDL, high-density lipoprotein; LDL, low-density lipoprotein: HOMA-IR, homeostasis model for assessment of insulin resistance.

Hepatic XO activity, oxidative stress, and inflammation markers

Hepatic XO activity in the febuxostat group was significantly suppressed compared to that in the fructose group (Fig. 3). The mRNA expression of the antioxidative response enzymes catalase (CAT) and glutathione peroxidase 1 (GPx-1) was significantly increased in the febuxostat group compared to that in the fructose group (Fig. 4A, B). The levels of MDA, a lipid peroxidation marker, were significantly suppressed in the febuxostat group compared to those in the fructose group (Fig. 4C). The mRNA expression of nicotinamide adenine dinucleotide phosphate oxidase 2 (NOX2) and cytochrome P450 2E1 (CYP2E1), enzymes related to oxidation, in the febuxostat group was not significantly different from those in the other groups. However, their mean values were lower than those of the fructose group (Fig. 4D, E). The mRNA expression of monocyte chemoattractant protein-1 (MCP-1) and tumor necrosis factor-α (TNF-α), which are inflammation markers, was significantly downregulated in the febuxostat group compared with that in the fructose group (Fig. 4F, G). Lastly, the mRNA expression of nuclear factor-kappa B (NFκB), an inflammation marker, did not differ significantly between the febuxostat and fructose groups (Fig. 4H).

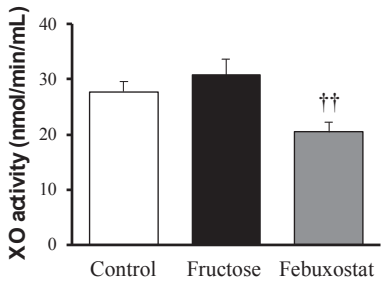

Fig. 3. Xanthine oxidase (XO) activity in the liver at 26 weeks of age. All data are shown as the mean ± SE; $n = 5$ in each group. * $p < 0.05$, ** $p < 0.01$ vs. control group; † $p < 0.05$, †† $p < 0.01$ vs. fructose group.

Pathological analysis in the liver

Macroscopic findings of the liver showed differences among the three groups. The color tone of the liver obtained from rats in the fructose group was whitish, whereas that of the liver obtained from rats in the febuxostat group was reddish (Fig. 5A). In addition, the asperity of the liver surface was improved in the febuxostat group compared with that in the fructose group (Fig. 5B). The liver weight corrected for tibia length did not show significant differences, with similar weights between the control and febuxostat groups (Fig. 5C). The liver pathology of each group was scored using NAS. As the control and fructose groups scored a total NAS greater than 5.0 points, the animals were determined to have NASH (Fig. 6A). Conversely, the febuxostat group was determined to have borderline NASH, as the total NAS was between 3.0 and 5.0 points (Fig. 6A). Similarly, the steatosis score of the febuxostat group was significantly lower than that of the fructose group (Fig. 6B). The hepatocyte ballooning scores did not show any significant differences between the groups. However, the lobular inflammation score in the febuxostat group was significantly lower than in the other two groups (Fig. 6B). The Ishak fibrosis stage in the febuxostat group was significantly lower than in the other two groups (Fig. 6C).

Based on Masson's trichrome staining, the control and fructose groups showed hepatic fibrosis and steatosis. In comparison, febuxostat treatment improved hepatic fibrosis and lipid accumulation (Fig. 7A, B). Quantitative analysis of the hepatic fibrosis area in the febuxostat group also showed a significant improvement compared to that in the fructose group (Fig. 7C). The hepatic triglyceride levels in the febuxostat group were significantly lower than those in the fructose group (Fig. 7D).

The AST and ALT levels in the febuxostat group were lower than those in the fructose group (Table 2). The uric acid level in the fructose group was the highest among the three groups; the levels in the febuxostat group were significantly lower than those in the fructose group (Table 2).

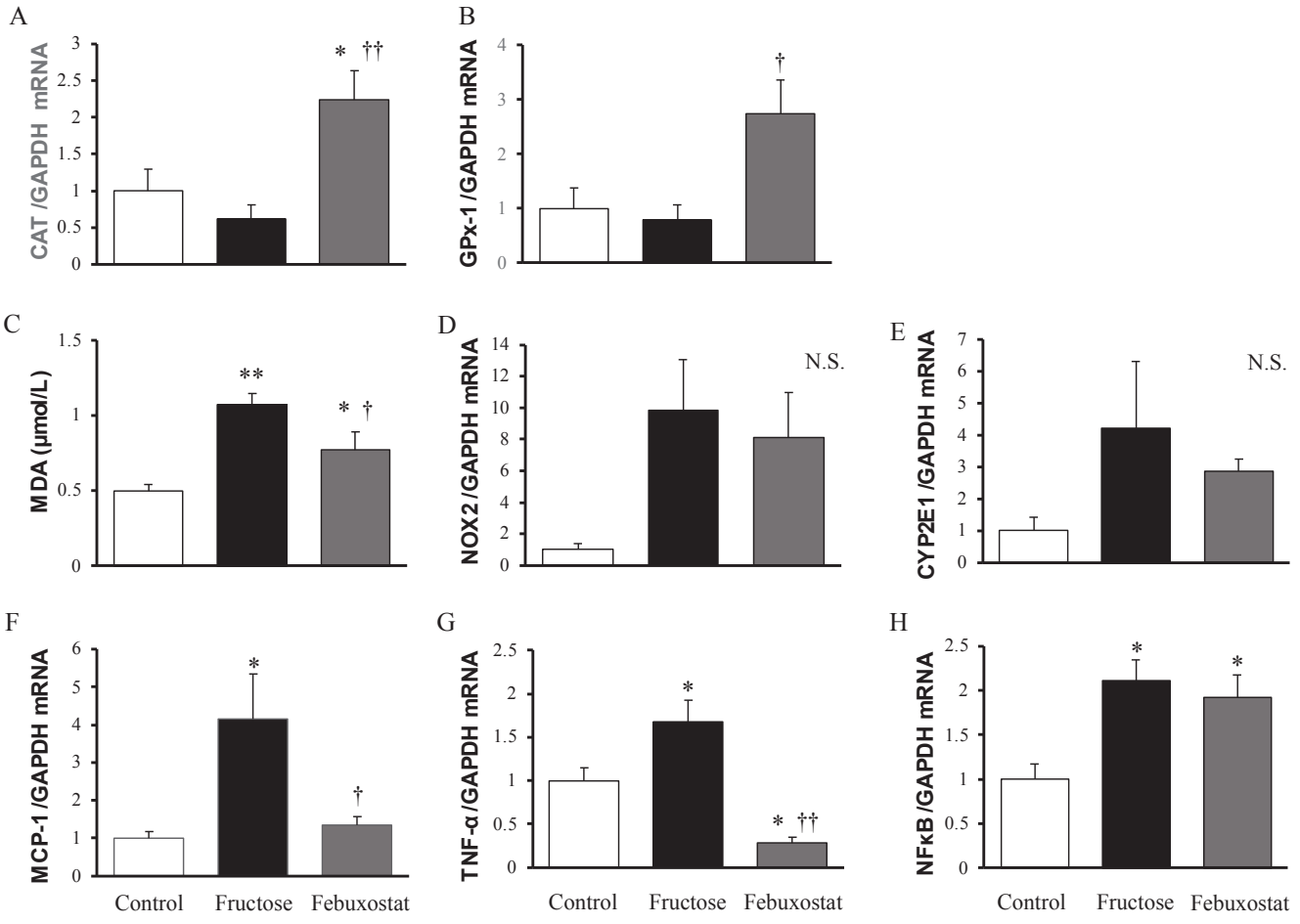

Fig. 4. Oxidant- and inflammation-related substances in the liver at 26 weeks of age. (**A**) mRNA levels of catalase (CAT). (**B**) mRNA levels of glutathione peroxidase (GPx-1). (**C**) Amount of malondialdehyde (MDA). (**D**) mRNA levels of nicotinamide adenine dinucleotide phosphate oxidase 2 (NOX2). (**E**) mRNA levels of cytochrome P450 2E1 (CYP2E1). (**F**) mRNA levels of monocyte chemoattractant protein-1 (MCP-1). (**G**) mRNA levels of tumor necrosis factor-α (TNF-α). (**H**) mRNA level of nuclear factor kappa B (NFκB). Glyceraldehyde 3-phosphate dehydrogenase (GAPDH) was used as an internal standard for (A, B) and (D–H). All data are shown as the mean ± SE; $n = 5$ in each group. * $p < 0.05$, ** $p < 0.01$ vs. control group; † $p < 0.05$, †† $p < 0.01$ vs. fructose group.

Mesenteric lipid deposition and aortic endothelial function

Oil Red O staining of mesenteric arteries showed greater lipid deposition in the fructose group than in the control group, and febuxostat decreased lipid deposition relative to that in the fructose group (Fig. 8A). Quantitative analysis of lipid deposition confirmed these observations (Fig. 8B). Aortic endothelial function in the febuxostat group was significantly improved to the same level as that in the control group (Fig. 8C).

Biochemical analyses revealed that the total HDL and LDL cholesterol levels in the plasma were significantly lower in the febuxostat group than those in the fructose group. In contrast, the LDL/HDL cholesterol ratio was significantly higher in the febuxostat group than in the fructose group (Table 2). Lastly, the plasma triglyceride levels in the febuxostat group were significantly lower than those in the fructose group (Table 2).

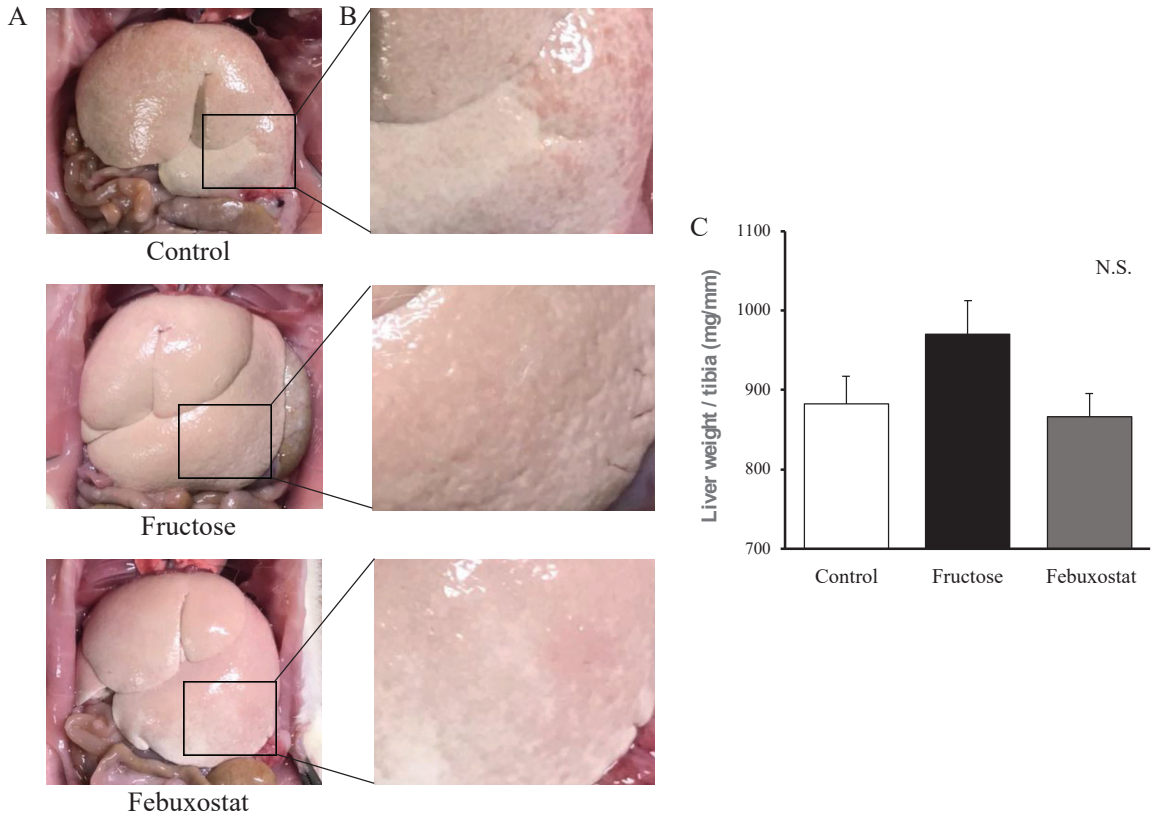

Fig. 5. Macroscopic findings and weight of the liver at 26 weeks of age. (**A**) Macroscopic findings in the liver. (**B**) Magnified photograph of the liver. (**C**) Liver weight corrected by tibia length. All data are shown as the mean ± SE; n = 5 in each group.

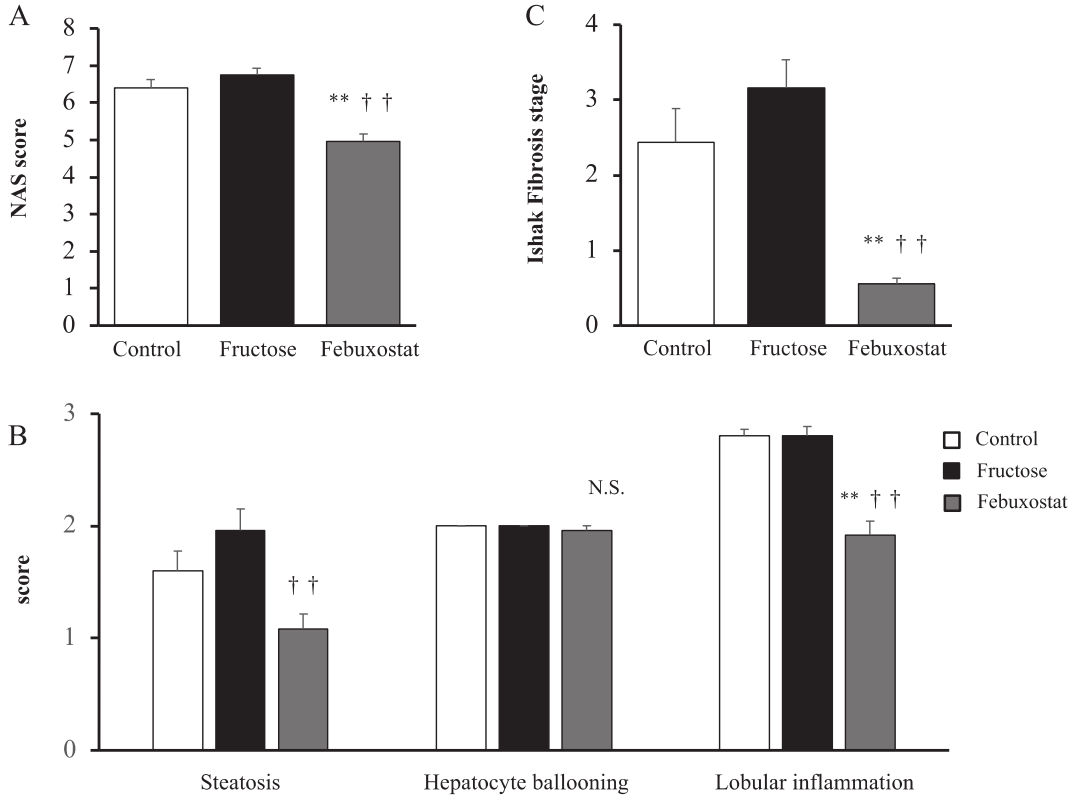

Fig. 6. Histological diagnosis of the liver. (**A**) NAFLD activity score (NAS). (**B**) Steatosis, hepatocyte ballooning, and lobular inflammation scores. (**C**) Ishak fibrosis stage. All data are shown as the mean ± SE; n = 5 in each group. ** $p < 0.01$ vs. control group; †† $p < 0.01$ vs. fructose group.

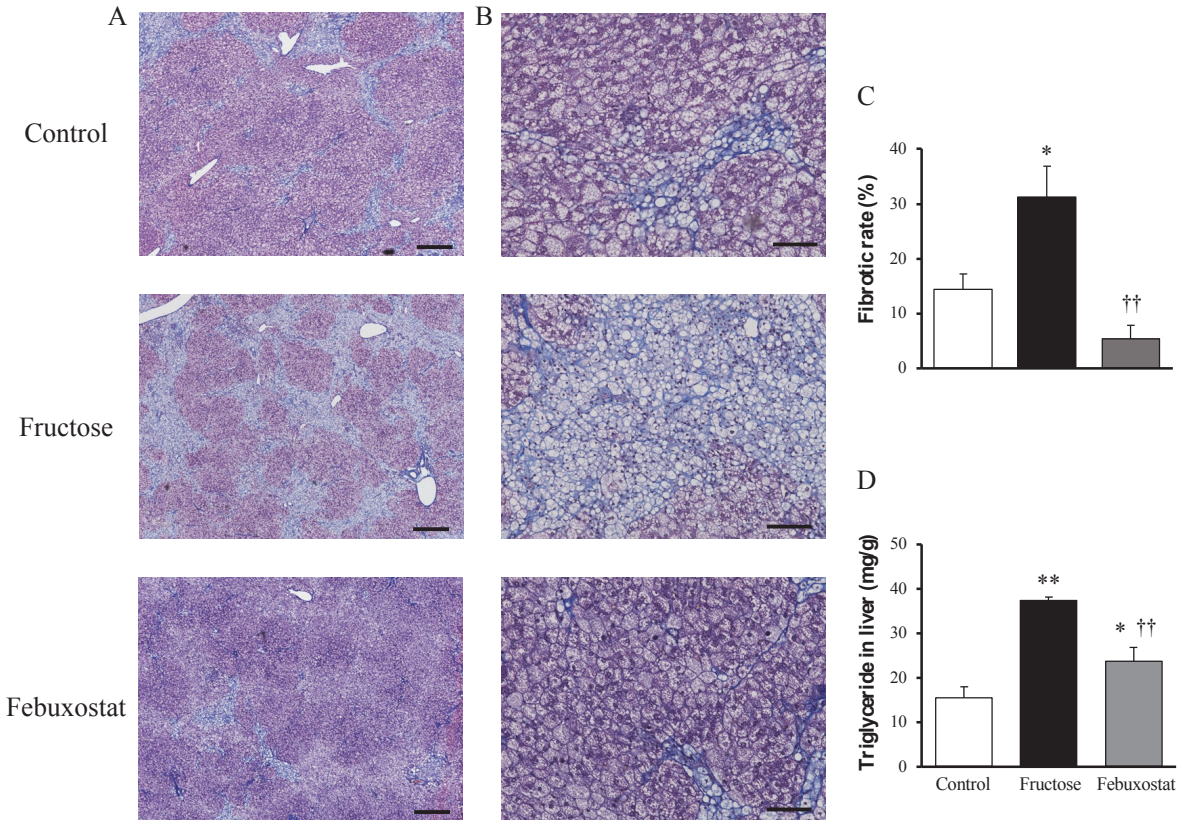

Fig. 7. Pathological findings in the liver at 26 weeks of age. (**A**) Masson's trichrome staining for hepatic fibrosis (magnification field ×4). Scale = 400 μm. (**B**) Masson's trichrome staining for hepatic fibrosis (magnification field ×20). Scale = 100 μm. (**C**) Hepatic fibrosis rate. (**D**) Triglycerides in the liver. All data are shown as the mean ± SE; $n = 5$ in each group. * $p < 0.05$, ** $p < 0.01$ vs. control group; †† $p < 0.01$ vs. fructose group.

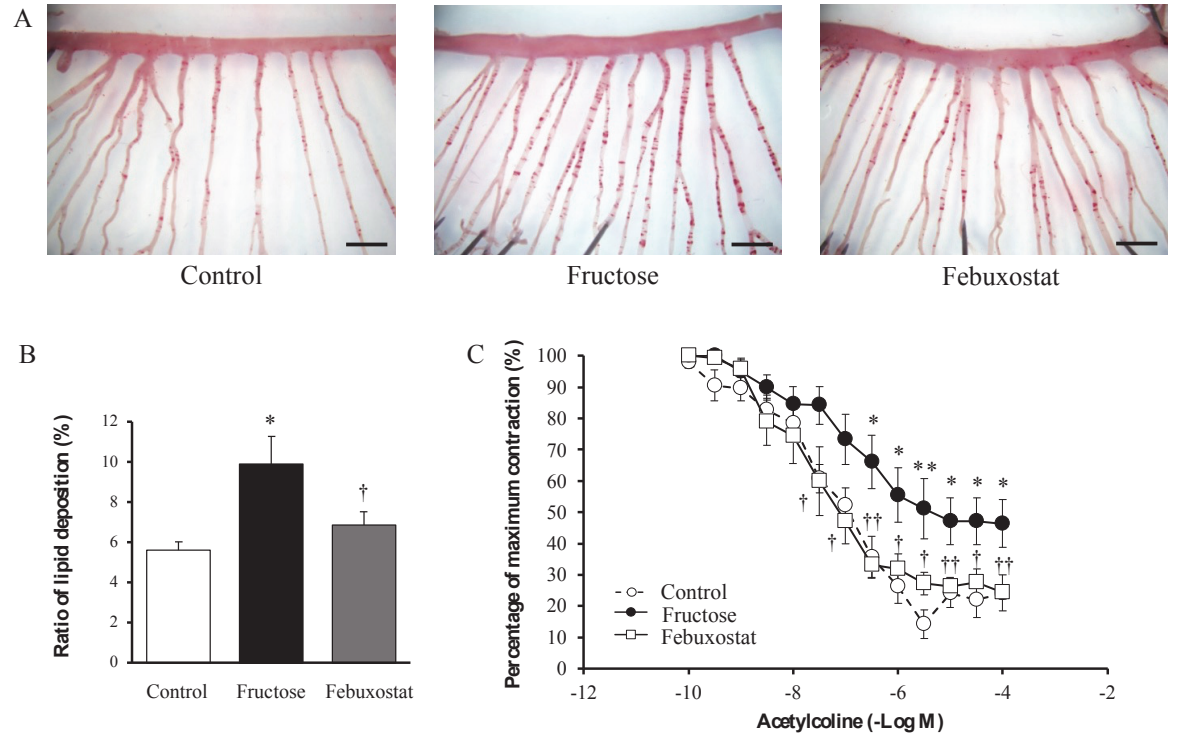

Fig. 8. Lipid deposition in the mesenteric artery branches and vascular endothelial function test at 26 weeks of age. (**A**) Isolated mesenteric arteries were stained with Oil Red O. Scale = 2 mm. (**B**) Lipid deposition rate in isolated mesenteric arteries. (**C**) Endothelium-dependent relaxation curve of aortic rings induced by acetylcholine (ACh). All data are shown as mean ± SE; $n = 5$ in each group. * $p < 0.05$, ** $p < 0.01$ vs. control group; † $p < 0.05$, †† $p < 0.01$ vs. fructose group.

Discussion

We examined the antioxidant effect of the XO inhibitor febuxostat against NASH and atherosclerosis in SHRSP5/Dmcr rats with elevated uric acid levels and oxidative stress induced by high fructose. These results suggest that febuxostat reduces uric acid and oxidative stress by inhibiting XO and may protect against NASH and atherosclerosis (Fig. 9).

We previously reported that SHRSP5/Dmcr rats fed an HFC diet developed NASH (Kitamori et al., 2012). In NASH, the liver becomes whitish and enlarged compared to a healthy liver. Pathological staining shows steatosis, hepatocyte ballooning, lobular inflammation, and hepatic fibrosis (Kleiner et al., 2005). In the present study, the control and fructose groups were determined to have NASH because their total NAS, based on steatosis, hepatocyte ballooning, and lobular inflammation, was greater than 5.0 points. Fructose loading induces significant hepatic hypertrophy, expansive steatosis, and fibrosis; this may be attributed to the rapid metabolism of fructose-to-fructose monophosphate. ATP is converted to ADP, which is then metabolized to AMP, inosine monophosphate, hypoxanthine, and xanthine (Vos and Lavine, 2013). The end products, uric acid and oxidative stress, cause inflammation and insulin resistance. High uric acid levels inhibit insulin receptor substrate-1 (IRS-1), which is involved in insulin signaling and directly induces insulin resistance (Zhu et al., 2014). Oxidative stress may involve TNF-α-induced impairment of insulin activity (Imoto et al., 2006). Moreover, insulin resistance can promote hepatic lipogenesis by increasing the release of free fatty acids by the adipose tissue and hyperglycemia/hyperinsulinemia (Finck, 2018). This suggests a profound relationship between NASH and glucose metabolism. Results from our glucose metabolism tests, namely the OGTT, ITT, fasting plasma glucose level, fasting plasma insulin level, and HOMA-IR, showed mild glucose intolerance and insulin resistance in the fructose group animals.

Our results demonstrated that febuxostat suppressed hepatic XO activity. XO catalyzes the sequential oxidation of hypoxanthine to xanthine and xanthine to uric acid and hydrogen peroxide. Therefore, the inhibition of XO activity reduces the production of uric acid and ROS generated during this process (Yisireyili et al., 2017). In the febuxostat group, uric acid levels were decreased, markers of oxidative reactive enzymes and lipid peroxidation were decreased, and markers of antioxidative response enzymes were increased compared to those in the fructose group. Febuxostat decreases uric acid levels and oxidative stress by inhibiting XO. Subsequently, this may exert protective effects on the liver by preventing the exacerbation of inflammation and insulin resistance (Fig. 9). The expression of inflammatory cytokine genes in the febuxostat group was downregulated compared to that in the fructose group, and insulin resistance was not observed. Pathological findings in the livers of febuxostat-treated animals showed no whitish color tone, low lipid accumulation, and hepatic fibrosis. According to the NAS, the febuxostat group was determined to have borderline NASH because the total NAS was between 3.0 and 4.0. Compared with the fructose group, the improved NAS in the febuxostat group may be attributed to the significant reduction in steatosis and suppression of lobular inflammation. Furthermore, the hepatic function was enhanced in the febuxostat group, as evaluated by lower AST and ALT levels than those in the fructose group. These results suggest that febuxostat inhibits the production of uric acid and ROS in the liver and suppresses insulin resistance, thereby reducing inflammation in the liver and preventing the worsening of NASH pathology. A previous study using NASH model mice showed that febuxostat exerted substantial protective effects against NASH related to steatohepatitis and inflammatory cytokine expression (Malik et al., 2011).

Vascular endothelial dysfunction is an early step in the development of atherosclerosis, after which cholesterol infiltrates the spaces between damaged endothelial cells, leading to the formation of atherosclerotic plaques, the progression

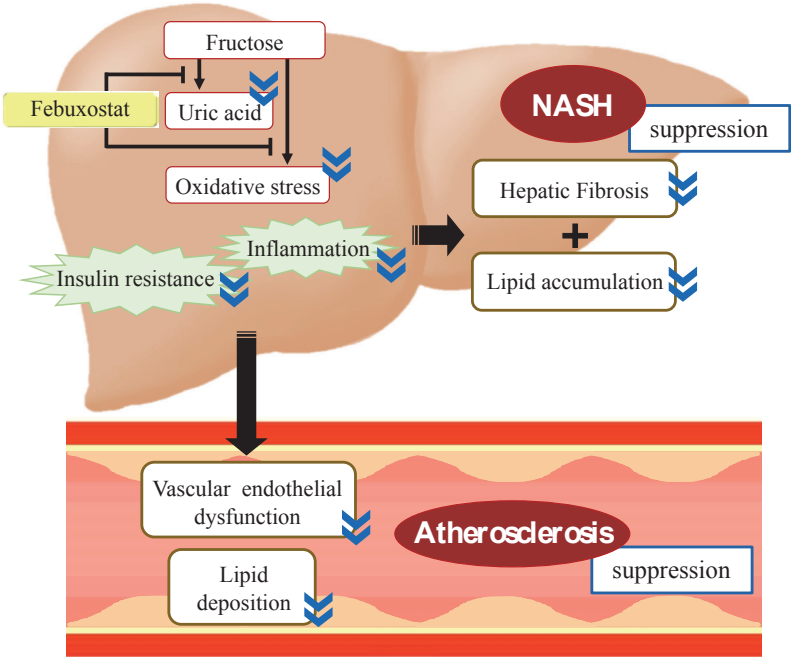

Fig. 9. Protective effect of XO inhibitor febuxostat on the liver and blood vascular system. NASH: non-alcoholic steatohepatitis.

of atherosclerosis, and complications associated with cardiovascular disease (Sitia et al., 2010). Nitric oxide (NO) released from vascular endothelial cells has a wide range of biological properties that maintain vascular homeostasis and plays a crucial role in normal endothelial function. These properties include modulation of vascular dilator tone, regulation of local cell growth, and protection of vessels from injurious consequences of platelets and cells circulating in the blood (Tousoulis et al., 2012). Therefore, the sufficient release of NO from vascular endothelial cells is important for the prevention of atherosclerosis. NO is involved in various pathways and has a crucial role in insulin signaling (Montagnani et al., 2001; Steinberg et al., 1994; Zeng et al., 2000). Insulin must first bind to and then activate the insulin receptor by phosphorylating key tyrosine residues on the β-subunit to function (Saltiel and Kahn, 2001). This results in the translocation of IRS-1 to the plasma membrane, where it interacts with the insulin receptor and undergoes tyrosine phosphorylation. This leads to the activation of phosphoinositide 3-kinase and protein kinase B (AKT), resulting in glucose transport into the cell, activation of NO synthase with arterial vasodilation, and stimulation of multiple intracellular metabolic processes (Defronzo, 2009; Schnyder et al., 2002; Zeng et al., 2000). However, in diabetes mellitus and hyperuricemia, which are associated with insulin resistance, the ability of insulin to phosphorylate tyrosine residues on IRS-1 is severely impaired, and the subsequent pathway is not activated (Defronzo, 2009). Therefore, the release of NO in endothelial dysfunction is impaired under these conditions, leading to atherosclerosis. In this study, compared to the fructose group, the endothelium-dependent acetylcholine response and NO-induced vasodilation were improved by febuxostat treatment. Furthermore, total cholesterol, LDL cholesterol, and blood triglyceride levels, which are directly related to atherosclerosis, were lower in the febuxostat group than in the fructose group. Although the mechanism by which febuxostat regulates blood lipids is unknown, febuxostat reduces lipid and cholesterol production, which is consistent with the results of the present study. Therefore, febuxostat may regulate lipid metabolism in the liver through antioxidant and anti-inflammatory mechanisms (Heikal et al., 2019; Malik et al., 2011; Wu et al., 2019). In the present study, Oil Red O staining of the mesenteric arteries revealed significant lipid deposition in the fructose group, whereas lipid deposition levels were reversed in the febuxostat group. This finding may be due to the synergistic effect of febuxostat on atherosclerosis, which reduces lipid and cholesterol synthesis and improves vascular endothelial function. In a clinical study, allopurinol, an XO inhibitor, improved endothelial function and prevented atherosclerosis progression in patients with chronic heart failure (George et al., 2006). Therefore, the findings of this study using the XO inhibitor, febuxostat, may represent phenomena similar to those reported for allopurinol.

Conclusions

The XO inhibitor febuxostat improved insulin resistance and inflammation in SHRSP5/Dmcr rats by reducing uric acid levels and oxidative stress and showed protective effects against NASH and atherosclerosis.

Acknowledgments
We would like to thank the Central Research Laboratory of Okayama University Medical School.

Animal rights
All rat experiments were performed in strict accordance with the recommendations of the standards related to the Care and Management of Laboratory Animals and Relief of Pain published by the Japanese Ministry of the Environment. The study protocol was approved by the Animal Experiment Committee of Okayama University (approval no. OKU-2020183).

Funding
This work was supported by grants from the Japan Society for the Promotion of Science (Grant Number 15K19178) and a Grant-in-Aid for Scientific Research (C) (Grant Number 18K10993) to S. Watanabe, and Gout Research Foundation of Japan to S. Watanabe.

Conflict of interests
The authors declare no conflict of interests directly relevant to the content of this article.

References

Argo CK, Caldwell SH (2009). Epidemiology and natural history of non-alcoholic steatohepatitis. Clin Liver Dis 13(4): 511–531. DOI: 10.1016/j.cld.2009.07.005.

Cohen JC, Horton JD, Hobbs HH (2011). Human fatty liver disease: old questions and new insights. Science 332(6037): 1519–1523. DOI: 10.1126/science.1204265.

Defronzo RA (2009). Banting Lecture. From the triumvirate to the ominous octet: a new paradigm for the treatment of type 2 diabetes mellitus. Diabetes 58(4): 773–795. DOI: 10.2337/db09-9028.

Elias J, Jr., Altun E, Zacks S, Armao DM, Woosley JT, Semelka RC (2009). MRI findings in nonalcoholic steatohepatitis: correlation with histopathology and clinical staging. Magn Reson Imaging 2 (7): 976–987. DOI: 10.1016/j.mri.2009.02.002.

Feig DI, Kang DH, Johnson RJ (2008). Uric acid and cardiovascular risk. N Engl J Med 359(17): 1811–1821. DOI: 10.1056/NEJMra0800885.

Finck BN (2018). Targeting Metabolism, Insulin Resistance, and Diabetes to Treat Nonalcoholic Steatohepatitis. Diabetes 67(12): 2485–2493. DOI: 10.2337/dbi18-0024.

George J, Carr E, Davies J, Belch JJ, Struthers A (2006). High-dose allopurinol improves endothelial function by profoundly reducing vascular oxidative stress and not by lowering uric acid. Circulation 114(23): 2508–2516. DOI:10.1161/circulationaha.106.651117.

Goodman ZD (2007). Grading and staging systems for inflammation and fibrosis in chronic liver diseases. J Hepatol 47(4): 598–607. DOI: 10.1016/j.jhep.2007.07.006.

Heikal MM, Shaaban AA, Elkashef WF, Ibrahim TM (2019). Effect of febuxostat on biochemical parameters of hyperlipidemia induced by a high-fat diet in rabbits. Can J Physiol Pharmacol 97(7): 611–622. DOI: 10.1139/cjpp-2018-0731.

Hosoo S, Koyama M, Kato M, Hirata T, Yamaguchi Y, Yamasaki H, et al. (2015). The Restorative Effects of *Eucommia ulmoides* Oliver Leaf Extract on Vascular Function in Spontaneously Hypertensive Rats. Molecules 20(12): 21971–21981. DOI: 10.3390/molecules201219826.

Imoto K, Kukidome D, Nishikawa T, Matsuhisa T, Sonoda K, Fujisawa K, et al. (2006). Impact of mitochondrial reactive oxygen species and apoptosis signal-regulating kinase 1 on insulin signaling. Diabetes 55(5): 1197–1204. DOI: 10.2337/db05-1187.

Ishak K, Baptista A, Bianchi L, Callea F, De Groote J, Gudat F, et al. (1995). Histological grading and staging of chronic hepatitis. J Hepatol 22(6): 696–699. DOI: 10.1016/0168-8278(95)80226-6.

Jegatheesan P, De Bandt JP (2017). Fructose and NAFLD: The Multifaceted Aspects of Fructose Metabolism. Nutrients 9(3): 230. DOI: 10.3390/nu9030230.

Khosla UM, Zharikov S, Finch JL, Nakagawa T, Roncal C, Mu W, et al. (2005). Hyperuricemia induces endothelial dysfunction. Kidney Int 67(5): 1739–1742. DOI: 10.1111/j.1523-1755.2005.00273.x.

Kitamori K, Naito H, Tamada H, Kobayashi M, Miyazawa D, Yasui Y, et al. (2012). Development of novel rat model for high-fat and high-cholesterol diet-induced steatohepatitis and severe fibrosis progression in SHRSP5/Dmcr. Environ Health Prev Med 17(3): 173–182. DOI: 10.1007/s12199-011-0235-9.

Kleiner DE, Brunt EM, Van Natta M, Behling C, Contos MJ, Cummings OW, et al. (2005). Design and validation of a histological scoring system for nonalcoholic fatty liver disease. Hepatology 41(6): 1313–1321. DOI: 10.1002/hep.20701.

Kumazaki S, Nakamura M, Sasaki S, Tagashira R, Maruyama N, Sato I, et al. (2019). Bile Acid Metabolism is an Intermediary Factor between Non-Alcoholic Steatohepatitis and Ischemic Heart Disease in SHRSP5/Dmcr Rats. J Nutr Food Sci 09(04). DOI: 10.35248/2155-9600.19.9.763.

Lin WT, Chan TF, Huang HL, Lee CY, Tsai S, Wu PW, et al. (2016). Fructose-Rich Beverage Intake and Central Adiposity, Uric Acid, and Pediatric Insulin Resistance. J Pediatr 171: 90–96.e91. DOI: 10.1016/j.jpeds.2015.12.061.

Malik UZ, Hundley NJ, Romero G, Radi R, Freeman BA, Tarpey MM, Kelley EE (2011). Febuxostat inhibition of endothelial-bound XO: implications for targeting vascular ROS production. Free Radic Biol Med 51(1): 179–184. DOI: 10.1016/j.freeradbiomed.2011.04.004.

Matsuura N, Nagasawa K, Minagawa Y, Ito S, Sano Y, Yamada Y, et al. (2015). Restraint stress exacerbates cardiac and adipose tissue pathology via β-adrenergic signaling in rats with metabolic syndrome. Am J Physiol Heart Circ Physiol 30(10): H1275–1286. DOI: 10.1152/ajpheart.00906.2014.

Mishima M, Hamada T, Maharani N, Ikeda N, Onohara T, Notsu T, et al. (2016). Effects of Uric Acid on the NO Production of HUVECs and its Restoration by Urate Lowering Agents. Drug Res (Stuttg) 66(5): 270–274. DOI: 10.1055/s-0035-1569405.

Montagnani M, Chen H, Barr VA, Quon MJ (2001). Insulin-stimulated activation of eNOS is independent of Ca2+ but requires phosphorylation by Akt at Ser(1179). J Biol Chem 276(32): 30392–30398. DOI: 10.1074/jbc.M103702200.

Mosca A, Nobili V, De Vito R, Crudele A, Scorletti E, Villani A, et al. (2017). Serum uric acid concentrations and fructose consumption are independently associated with NASH in children and adolescents. J Hepatol 66(5): 1031–1036. DOI: 10.1016/j.jhep.2016.12.025.

Nakatsu Y, Seno Y, Kushiyama A, Sakoda H, Fujishiro M, Katasako A, et al. (2015). The xanthine oxidase inhibitor febuxostat suppresses development of nonalcoholic steatohepatitis in a rodent model. Am J Physiol Gastrointest Liver Physiol 309(1): G42–51. DOI: 10.1152/ajpgi.00443.2014.

Ndrepepa G (2018). Uric acid and cardiovascular disease. Clin Chim Acta 484: 150–163. DOI: 10.1016/j.cca.2018.05.046.

Nosrati N, Aghazadeh S, Yazdanparast R (2010). Effects of *Teucrium polium* on Insulin Resistance in Nonalcoholic Steatohepatitis. J Acupunct Meridian Stud 3(2): 104–110. DOI: 10.1016/s2005-2901(10)60019-2.

Saltiel AR, Kahn CR (2001). Insulin signalling and the regulation of glucose and lipid metabolism. Nature 414(6865): 799–806. DOI: 10.1038/414799a.

Schnyder B, Pittet M, Durand J, Schnyder-Candrian S (2002). Rapid effects of glucose on the insulin signaling of endothelial NO generation and epithelial Na transport. Am J Physiol Endocrinol Metab 282(1): E87–94. DOI: 10.1152/ajpendo.00050.2001.

Shuprovych AA, Hurina NM, Korpacheva-Zinych OV (2011). [Disorders of uric acid metabolism in rats with fructose-induced experimental insulin resistance syndrome]. Fiziol Zh 57(1): 72–81.

Sitia S, Tomasoni L, Atzeni F, Ambrosio G, Cordiano C, Catapano A, et al. (2010). From endothelial dysfunction to atherosclerosis. Autoimmun Rev 9(12): 830–834. DOI: 10.1016/j.autrev.2010.07.016.

Softic S, Cohen DE, Kahn CR (2016). Role of Dietary Fructose and Hepatic De Novo Lipogenesis in Fatty Liver Disease. Dig Dis Sci 61(5): 1282–1293. DOI: 10.1007/s10620-016-4054-0.

Steinberg HO, Brechtel G, Johnson A, Fineberg N, Baron AD (1994). Insulin-mediated skeletal muscle vasodilation is nitric oxide dependent. A novel action of insulin to increase nitric oxide release. J Clin Invest 94(3): 1172–1179. DOI: 10.1172/jci117433.

Tousoulis D, Kampoli AM, Tentolouris C, Papageorgiou N, Stefanadis C (2012). The role of nitric oxide on endothelial function. Curr Vasc Pharmacol 10(1): 4–18. DOI: 10.2174/157016112798829760.

Verdecchia P, Schillaci G, Reboldi G, Santeusanio F, Porcellati C, Brunetti P (2000). Relation between serum uric acid and risk of cardiovascular disease in essential hypertension. The PIUMA study. Hypertension 36(6): 1072–1078. DOI: 10.1161/01.hyp.36.6.1072.

Vos MB, Lavine JE (2013). Dietary fructose in nonalcoholic fatty liver disease. Hepatology 57(6): 2525–2531. DOI: 10.1002/hep.26299.

Watanabe S, Kumazaki S, Kusunoki K, Inoue T, Maeda Y, Usui S, et al. (2018). A High-Fat and High-Cholesterol Diet Induces Cardiac Fibrosis, Vascular Endothelial, and Left Ventricular Diastolic Dysfunction in SHRSP5/Dmcr Rats. J Atheroscler Thromb 25(5): 439–453. DOI: 10.5551/jat.40956.

Wei J, Lin Y, Li Y, Ying C, Chen J, Song L, et al. (2011). Perinatal exposure to bisphenol A at reference dose predisposes offspring to metabolic syndrome in adult rats on a high-fat diet. Endocrinology 152(8): 3049–3061. DOI: 10.1210/en.2011-0045.

Wei JL, Leung JC, Loong TC, Wong GL, Yeung DK, Chan RS, et al. (2015). Prevalence and Severity of Nonalcoholic Fatty Liver Disease in Non-Obese Patients: A Population Study Using Proton-Magnetic Resonance Spectroscopy. Am J Gastroenterol 110(9): 1306–1314; quiz 1315. DOI: 10.1038/ajg.2015.235.

Wu J, Zhang YP, Qu Y, Jie LG, Deng JX, Yu QH (2019). Efficacy of uric acid-lowering therapy on hypercholesterolemia and hypertriglyceridemia in gouty patients. Int J Rheum Dis 22(8): 1445–1451. DOI: 10.1111/1756-185x.13652.

Xu D, Murakoshi N, Tajiri K, Duo F, Okabe Y, Murakata Y, et al. (2021). Xanthine oxidase inhibitor febuxostat reduces atrial fibrillation susceptibility by inhibition of oxidized CaMKII in Dahl salt-sensitive rats. Clin Sci (Lond) 135(20): 2409–2422. DOI: 10.1042/cs20210405.

Yisireyili M, Hayashi M, Wu H, Uchida Y, Yamamoto K, Kikuchi R, et al. (2017). Xanthine oxidase inhibition by febuxostat attenuates stress-induced hyperuricemia, glucose dysmetabolism, and prothrombotic state in mice. Sci Rep 7(1): 1266. DOI: 10.1038/s41598-017-01366-3.

Zeng G, Nystrom FH, Ravichandran LV, Cong LN, Kirby M, Mostowski H, Quon MJ (2000). Roles for insulin receptor, PI3-kinase, and Akt in insulin-signaling pathways related to production of nitric oxide in human vascular endothelial cells. Circulation 101(13): 1539–1545. DOI: 10.1161/01.cir.101.13.1539.

Zhang W, Iso H, Murakami Y, Miura K, Nagai M, Sugiyama D, et al. (2016). Serum Uric Acid and Mortality Form Cardiovascular Disease: EPOCH-JAPAN Study. J Atheroscler Thromb 23(6): 692–703. DOI: 10.5551/jat.31591.

Zhu Y, Hu Y, Huang T, Zhang Y, Li Z, Luo C, et al. (2014). High uric acid directly inhibits insulin signalling and induces insulin resistance. Biochem Biophys Res Commun 447(4): 707–714. DOI: 10.1016/j.bbrc.2014.04.080.